Inorg. Chem. **2002**, *41*, 5716–5720

New Layered Rubidium Rare-Earth Selenides: Syntheses, Structures, Physical Properties, and Electronic Structures for $RbLnSe_2$

Bin Deng, Donald E. Ellis, and James A. Ibers*

Department of Chemistry and Department of Physics and Astronomy, Northwestern University, 2145 Sheridan Road, Evanston, Illinois 60208-3113

Received May 7, 2002

The compounds $RbLnSe_2$ (Ln = La, Ce, Pr, Nd, Sm, Gd, Tb, Ho, Er, Lu) have been synthesized by means of the reactive flux method at 1173 K. These isostructural compounds, which have the α-$NaFeO_2$ structure type, crystallize with three formula units in space group D_{3d}^5-$R\bar{3}m$ of the trigonal system in cells at T = 153 K of dimensions (a, c in Å) La, 4.4313(4), 23.710(3); Ce, 4.3873(3), 23.656(3); Pr, 4.3524(11), 23.655(7); Nd, 4.3231(5), 23.670(4); Sm, 4.2799(4), 23.647(3); Gd, 4.2473(7), 23.689(5); Tb, 4.2197(4), 23.631(3); Ho, 4.1869(6), 23.652(5); Er, 4.1541(8), 23.576(7); Lu, 4.1294(6), 23.614(5). The structure consists of close-packed Se layers in a pseudocubic structure distorted along [111]. The Rb and Ln atoms occupy distorted octahedral sites in alternating layers. The Rb-centered octahedra share edges with the Ln-centered octahedra between layers. Within a given layer, both the Rb-centered and Ln-centered octahedra share edges with themselves. $RbTbSe_2$ and $RbErSe_2$ exhibit Curie–Weiss paramagnetism between 5 and 300 K, and $RbCeSe_2$ exhibits Curie–Weiss paramagnetism between 100 and 300 K. The optical transitions for $RbCeSe_2$, $RbTbSe_2$, and $RbErSe_2$ are in the 2.0–2.2 eV region of the spectrum, both from diffuse reflectance spectra and from first-principles calculations. These calculations also provide insight into the electronic structures and chemical bonding in $RbLnSe_2$. A quadratic fit for the lanthanide contraction of the Ln–Se distance is superior to the linear one only if the closed-shell atoms La and Lu are included.

Introduction

Many ternary chalcogenides $A^IM^{III}Q_2$ (Q = S, Se, Te), where A = alkali metal or Cu, M = transition metal or rare-earth element, crystallize in the α-$NaFeO_2$ structure type. Some of these materials have attracted attention for practical reasons, namely in battery[1−4] and luminescence applications,[5] but also for fundamental reasons, especially for the interesting magnetic coupling between layers.[6−8] Because A, M, and Q can be varied systematically over a wide range within this structure type, potentially their physical properties can also be tuned. Previous research has focused principally on systems with A = Li, M = transition metal.

Consider now M = rare-earth, herein denoted Ln. Work in this area has focused on synthesis and structure as opposed to physical properties. Many $ALnS_2$ compounds have been synthesized and their crystal structures determined by powder or single-crystal diffraction methods.[9−15] Results for the selenides and especially the tellurides are more limited: the structures of $LiLnSe_2$ and $NaLnSe_2$ (Ln = La, Ce, Nd, Sm, Gd, Tb, Dy, Ho, Er, Y)[7] have been determined from powders, whereas the structures of $KCeSe_2$,[16] $KSmTe_2$,[14] and $KErTe_2$[17]

* To whom correspondence should be addressed. E-mail: ibers@chem.northwestern.edu.

(1) Bruce, P. G. *J. Chem. Soc., Chem. Commun.* **1997**, 1817−1824.
(2) Manthiram, A.; Kim, J. *Chem. Mater.* **1998**, *10*, 2895−2909.
(3) Vincent, C. A. *Solid State Ionics* **2000**, *134*, 159−167.
(4) Ammundsen, B.; Paulsen, J. *Adv. Mater.* **2001**, *13*, 943−956.
(5) Yocom, P. N.; Dismukes, J. P. U.S. Patent 3981819, 1976.
(6) Goodenough, J. B. *Prog. Solid State Chem.* **1971**, *5*, 145−399.
(7) Ohtani, T.; Honjo, H.; Hironobu, W. *Mater. Res. Bull.* **1987**, *22*, 829−840.
(8) Dutta, G.; Manthiram, A.; Goodenough, J. B.; Grenier, J.-C. *J. Solid State Chem.* **1992**, *96*, 123−131.
(9) Ballestracci, R.; Bertaut, E. F. *Bull. Soc. Fr. Mineral. Cristallogr.* **1964**, *87*, 512−517.
(10) Ballestracci, R. *Bull. Soc. Fr. Mineral. Cristallogr.* **1965**, *88*, 207−210.
(11) Bronger, W.; Elter, R.; Maus, E.; Schmitt, T. *Rev. Chim. Miner.* **1973**, *10*, 147−150.
(12) Sato, M.; Adachi, G.; Shiokawa, J. *Mater. Res. Bull.* **1984**, *19*, 1215−1220.
(13) Schleid, T.; Lissner, F. *Eur. J. Solid State Inorg. Chem.* **1993**, *30*, 829−836.
(14) Bronger, W.; Brüggemann, W.; von der Ahe, M.; Schmitz, D. *J. Alloys Compd.* **1993**, *200*, 205−210.
(15) Bronger, W.; Eyck, J.; Kruse, K.; Schmitz, D. *Eur. J. Solid State Inorg. Chem.* **1996**, *33*, 213−226.
(16) Plug, C. M.; Verschoor, G. C. *Acta Crystallogr., Sect. B* **1976**, *32*, 1856−1858.

10.1021/ic020324j CCC: $22.00
Published on Web 10/05/2002

Table 1. Crystal Data and Structure Refinements for $RbLnSe_2$[a]

cmpd	$RbLaSe_2$	$RbCeSe_2$	$RbPrSe_2$	$RbNdSe_2$	$RbSmSe_2$	$RbGdSe_2$	$RbTbSe_2$	$RbHoSe_2$	$RbErSe_2$	$RbLuSe_2$
fw	382.30	383.51	384.30	387.63	393.74	400.64	402.31	408.32	410.65	418.36
a (Å)	4.4313(4)	4.3873(3)	4.3524(11)	4.3231(5)	4.2799(4)	4.2473(7)	4.2197(4)	4.1869(6)	4.1541(8)	4.1294(6)
c (Å)	23.710(3)	23.656(3)	23.655(7)	23.670(4)	23.647(3)	23.689(5)	23.631(3)	23.652(5)	23.576(7)	23.614(5)
V (Å^3)	403.20(7)	394.34(6)	388.07(18)	383.11(9)	375.12(6)	370.09(12)	364.39(7)	359.08(11)	352.33(14)	348.72(10)
ρ_c (g cm^{-3})	4.723	4.845	4.933	5.040	5.229	5.393	5.500	5.665	5.806	5.976
μ (cm^{-1})	303.0	315.1	326.4	336.9	357.7	377.9	392.9	416.2	434.4	470.8
x_1[c]	0.04	0.02	0.01	0.04	0.04	0.03	0.04	0.04	0.05	0.03
R (F)[b]	0.0236	0.0156	0.0226	0.0233	0.0294	0.0197	0.0240	0.0252	0.0335	0.0222
R_w (F_o^2)[c]	0.0596	0.0381	0.0437	0.0623	0.0792	0.0524	0.0705	0.0694	0.0852	0.0607

[a] For all structures, $Z = 3$, space group $= R\bar{3}m$, $T = 153(2)$ K, and $\lambda = 0.71073$ Å. [b] $R(F) = \sum||F_o| - |F_c||/|F_o|$ for $F_o^2 > 2\sigma(F_o^2)$. [c] $R_w(F_o^2) = \{\sum[w(F_o^2 - F_c^2)^2]/wF_o^4\}^{1/2}$ for all data. $w^{-1} = \sigma^2(F_o^2) + (x_1 \times F_o^2)^2$ for $F_o^2 \geq 0$, and $w^{-1} = \sigma^2(F_o^2)$ for $F_o^2 < 0$.

have been determined from single crystals. Here, we report the syntheses of 10 members of the $RbLnSe_2$ family, together with details on crystal structures, magnetic properties, optical properties, and first principles calculations.

Experiment Details

Syntheses. The following reactants were used as received: La (Reacton, 99.9%), Ce (Reacton, 99.9%), Pr (Aldrich, 99.9%), Nd (Strem, 99.9%), Sm (Alfa, 99.9%), Gd (Alfa, 99.9%), Tb (Alfa, 99.9%), Ho (Alfa, 99.9%), Er (Strem, 99.9%), Lu (Strem, 99.9%), Rb (Aldrich, 98%), Se (Alfa, 99.5%), RbI (Strem, 99%). Rb_2Se_3, the reactive flux[18,19] in the syntheses, was prepared by the stoichiometric reaction of the elements in liquid NH_3. All ternary rubidium rare-earth selenides were prepared by the reaction of 0.5 mmol of Ln, 1.0 mmol of Se, 0.4 mmol of Rb_2Se_3 (in excess), and 250 mg of RbI. The samples were loaded into fused-silica tubes under an argon atmosphere in a glovebox. These tubes were evacuated to about 10^{-4} Torr and sealed, and then placed in a computer-controlled furnace. The samples were heated to 1173 K in 20 h, kept at 1173 K for 3 days, cooled at 3 K/h to 373 K, and then cooled to 298 K. The products were washed with deionized water and dried with methanol. Analysis of these compounds with an EDX-equipped Hitachi S-3500 SEM showed the presence of Rb, Ln, and Se. These compounds are stable in air for at least one week.

Structure Determinations. Single-crystal X-ray diffraction data were obtained with the use of graphite-monochromatized Mo Kα radiation ($\lambda = 0.71073$ Å) at 153 K on a Bruker Smart-1000 CCD diffractometer.[20] The crystal-to-detector distance was 5.023 cm. Data were collected by a scan of 0.3° in ω in groups of 606 frames for each of the φ settings 0°, 90°, 180°, and 270° for $RbCeSe_2$, $RbPrSe_2$, $RbNdSe_2$, and $RbSmSe_2$; in groups of 606 frames for each of the φ settings 0°, 120°, and 240° for $RbLaSe_2$, $RbGdSe_2$, $RbTbSe_2$, $RbHoSe_2$, and $RbLuSe_2$; and by a scan of 0.25° in ω in groups of 727 frames for each of the φ settings 0°, 120°, and 240° for $RbErSe_2$. Intensity data were collected with the program SMART.[20] Cell refinement and data reduction were carried out with the use of the program SAINT,[20] and face-indexed absorption corrections were performed numerically with the use of the program XPREP.[21] Then, the program SADABS[20] was employed to make incident beam and decay corrections. The structures were solved with the direct-methods program SHELXS and refined with the full-matrix least-squares program SHELXL.[21] Each final refinement included anisotropic displacement parameters and a secondary extinction correction. Additional experimental details are shown in Table 1 and in Supporting Information.

Magnetic Susceptibility Measurements. Measurements on crystals of $RbCeSe_2$ (52.0 mg), $RbTbSe_2$ (57.0 mg), and $RbErSe_2$ (71.1 mg) were carried out with the use of a Quantum Design SQUID magnetometer (MPMSS Quantum Design). The samples were loaded into gelatin capsules. Zero-field cooled susceptibility data were collected between 5 and 300 K at an applied field of 1000 G. The susceptibility data in the temperature range 100−300 K were fit by a least-squares procedure to the Curie−Weiss equation $\chi = C/(T - \theta_p)$, where C is the Curie constant and θ_p is the Weiss constant. The effective moment (μ_{eff}) was calculated from the equation $\mu_{eff} = (7.997C)^{1/2}\mu_B$.[22]

Diffuse Reflectance Spectroscopy. A Cary 1E UV−vis spectrophotometer with a diffuse reflectance accessory was used to measure the diffuse reflectance spectra of the compounds $RbCeSe_2$, $RbTbSe_2$, and $RbErSe_2$ over the range 350 nm (3.54 eV) to 900 nm (1.38 eV) at 20 °C. The absorption (α/S) data were calculated from these measurements with the use of the Kubelka−Munk function[23,24] $\alpha/S = (1 - R)^2/2R$, where R is the reflectance at a given energy, α is the absorption coefficient, and S is the scattering coefficient.

TB-LMTO Calculations. Electronic structures were calculated by means of the self-consistent, scalar relativistic linearized muffin-tin orbital program of Andersen and co-workers[25−27] within the atomic sphere approximation (ASA). This method splits the crystal space into overlapping atomic spheres (Wigner−Seitz spheres) whose radii are chosen to fill the crystal volume completely. In the calculations presented here, the von Barth−Hedin exchange-correlation potential was used within the local density approximation (LDA).[28] All k-space integrations were performed with the tetrahedron method.[29,30] The basis sets consisted of the valence 5s electrons for Rb; 6s, 5p, and 5d for Ln; 4s and 4p for Se; and 1s for empty spheres. The 4f-electrons were treated as core states.

(17) Keane, P. M.; Ibers, J. A. *Acta Crystallogr., Sect. C.* **1992**, *48*, 1301−1303.
(18) Sunshine, S. A.; Kang, D.; Ibers, J. A. *J. Am. Chem. Soc.* **1987**, *109*, 6202−6204.
(19) Pell, M. A.; Ibers, J. A. *Chem. Ber.* **1997**, *130*, 1−8.
(20) *SMART Version 5.054 Data Collection and SAINT-Plus Version 6.22 Data Processing Software for the SMART System*; Bruker Analytical X-ray Instruments, Inc.: Madison, WI, 2000.
(21) Sheldrick, G. M. *SHELXTL DOS/Windows/NT Version 6.12*; Bruker Analytical X-ray Instruments, Inc.: Madison, WI, 2000.
(22) O'Connor, C. J. *Prog. Inorg. Chem.* **1982**, *29*, 203−283.
(23) Kortüm, G. *Reflectance Spectroscopy. Principles, Methods, Applications*; Springer-Verlag: New York, Inc.: New York, 1969.
(24) Tandon, S. P.; Gupta, J. P. *Phys. Status Solidi A* **1970**, *37*, 43−45.
(25) Andersen, O. K. *Phys. Rev. B* **1975**, *12*, 3060−3083.
(26) Andersen, O. K.; Jepsen, O. *Phys. Rev. Lett.* **1984**, *53*, 2571−2574.
(27) Jepsen, O.; Andersen, O. K. *Z. Phys. B: Condens. Matter* **1995**, *97*, 35−47.
(28) Hedin, L.; Lundqvist, B. I. *J. Phys. Chem. Solids* **1971**, *4*, 2064−2083.
(29) Lambrecht, W. R. L.; Andersen, O. K. *Phys. Rev. B* **1986**, *34*, 2439−2449.
(30) Jepsen, O.; Andersen, O. K. *Solid State Commun.* **1971**, *9*, 1763−1767.

Table 2. Selected Bond Lengths (Å) and Angles (deg) for $RbLnSe_2$

cmpd	$RbLaSe_2$	$RbCeSe_2$	$RbPrSe_2$	$RbNdSe_2$	$RbSmSe_2$	$RbGdSe_2$	$RbTbSe_2$	$RbHoSe_2$	$RbErSe_2$	$RbLuSe_2$
Rb−Se × 6	3.4599(8)	3.4471(5)	3.4370(9)	3.4320(8)	3.4148(2)	3.4128(8)	3.4042(8)	3.3976(9)	3.3819(11)	3.3814(9)
Ln-Se × 6	3.0295(6)	2.9986(4)	2.9778(7)	2.9591(6)	2.9353(2)	2.9142(7)	2.8934(6)	2.8741(7)	2.8530(9)	2.8371(7)
Se−Rb−Se	79.64(2)	79.04(1)	78.57(2)	78.07(2)	77.61(1)	76.96(2)	76.60(2)	76.07(2)	75.78(3)	75.27(2)
Se-Ln-Se	86.00(2)	85.96(2)	86.09(2)	86.15(2)	86.39(1)	86.44(2)	86.36(3)	86.50(3)	86.56(3)	86.60(3)

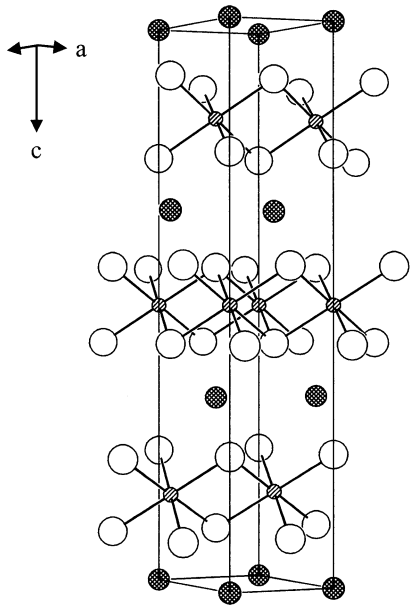

Figure 1. Crystal structure of $RbLaSe_2$ as viewed along [310]. The large open circles are Se, the medium crosshatched circles are Rb, and the small striped circles are La.

The 5p- and 5d-electrons for Rb, 4d for Se, and p−d states for empty spheres were downfolded by means of the technique described by Löwdin.[31] The crystal orbital Hamiltonian population (COHP),[32] which is the density of states weighted by the corresponding Hamiltonian matrix element, was calculated in order to analyze the strength and nature of the bonding. Within the Brillouin zone, 457 irreducible *k* points were used. The high-symmetry points are Γ(0, 0, 0), Z($^1/_2$, $^1/_2$, $^1/_2$), F($^1/_2$, $^1/_2$, 0), and L(0, $^1/_2$, 0) in terms of the reciprocal basis vectors.[33]

Results and Discussion

Syntheses and Structure. The compounds $RbLnSe_2$ (Ln = La, Ce, Pr, Nd, Sm, Gd, Tb, Ho, Er, Lu) have been synthesized by means of the reactive flux method at 1173 K. These compounds are isostructural, possessing the α-$NaFeO_2$ structure type. The structure of $RbLaSe_2$ is shown in Figure 1. It consists of close-packed Se layers in a pseudocubic structure distorted along the [111] direction. The Rb and Ln ions are situated in alternating layers and have distorted octahedral coordination. The Rb-centered octahedra share edges with the Ln-centered octahedra between layers. Within the same layer, both the Rb-centered and Ln-centered octahedra share edges with themselves. Table 2 lists important metrical parameters for this series of compounds. The distorted octahedra are compressed along [001] for Ln-centered octahedra and elongated for Rb-centered octahedra. The Rb−Se and Ln−Se distances in these compounds are reasonable. For example, Rb−Se distances decrease monotonically from 3.4599(8) Å (La) to 3.3814(9) (Lu) Å. These are comparable with those in Rb_2Se_5 (3.36(1) to 3.89(2) Å).[34] Ln−Se distances decrease monotonically from 3.0295(6) Å (La) to 2.8371(7) (Lu) Å, compared with those of 2.826 to 3.019 Å in $BaLnCuSe_3$ and $LiLnSe_2$ (six-coordinated).[7, 35]

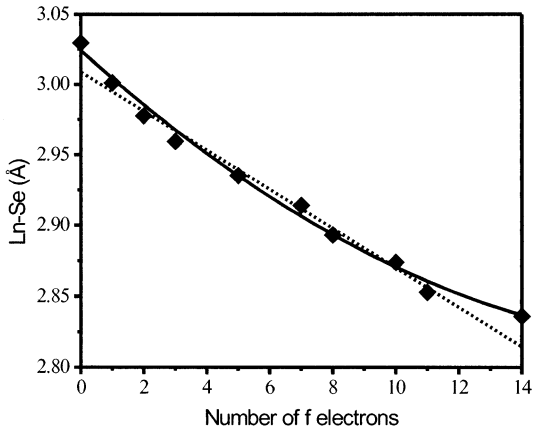

Figure 2. Ln−Se bond distances (Å) in $RbLnSe_2$ vs the number of f-electrons. The dashed line is the linear least-squares fit, and the solid line is the quadratic least-squares fit for $0 \le n \le 14$.

Lanthanide Contraction. Both the lattice constants and the bond distances clearly reflect the consequence of the lanthanide contraction. Recently, Quadrelli[36] showed from an examination of structural results for the isotypical compounds $[Ln(OH_2)_9][EtOSO_3]_3$ and $[Ln(OH_2)_9][CF_3SO_3]_3$ that improved fits to the contraction over the f-block of the Ln−O distances are obtained by use of a quadratic expression $d(\text{Ln−O}) = A_0 - A_1n + A_2n^2$, where $0 \le n \le 14$ is the number of f-electrons. In other words, the usual linear expression has been embellished with a quadratic term. Figure 2 suggests that a similar quadratic fit of d(Ln−Se) versus n for the present isostructural $RbLnSe_2$ compounds is superior to the usual linear one. However, if the closed-shell atoms La and Lu are excluded, that is, if $1 \le n \le 13$, then the quadratic fit is not superior to a linear one $d(\text{Ln−Se}) = B_0 - B_1n$, as can be surmised from the data in Table 3. The nonlinear relationship noted by Quadrelli[36] was actually described in much earlier work[37,38] where it was ascribed to crystal-field contractions of those rare-earths

(31) Löwdin, P.-O. *J. Chem. Phys.* **1951**, *19*, 1396−1401.
(32) Dronskowski, R.; Blöchl, P. E. *J. Phys. Chem.* **1993**, *97*, 8617−8624.
(33) Bradley, C. J.; Cracknell, A. P. *The Mathematical Theory of Symmetry in Solids. Representation theory for point groups and space groups*; Clarendon Press: Oxford, 1972.
(34) Böttcher, P. *Z. Kristallogr.* **1979**, *150*, 65−73.
(35) Christuk, A. E.; Wu, P.; Ibers, J. A. *J. Solid State Chem.* **1994**, *110*, 330−336.
(36) Quadrelli, E. A. *Inorg. Chem.* **2002**, *41*, 167−169.
(37) Gschneidner, K. A., Jr.; Valletta, R. M. *Acta Metall.* **1968**, *16*, 477−484.
(38) Beaudry, B. J.; Gschneidner, K. A., Jr. In *Handbook on the Physics and Chemistry of Rare Earths*, Gschneidner, Jr., K. A.; Eyring, L. R., Eds.; North-Holland Publishing Co.: Amsterdam, 1978; Vol. 1, Chapter 2.

Table 3. Least-Squares Fits of Ln−Se Distances Versus Number of f-Electrons

type	A_0 or B_0 (Å)	A_1 or B_1 (Å)	A_2 (Å)	R^2 (%)	comment
quadratic[a]	3.021(5)	0.0198(17)	0.00048(12)	99.2	La, Lu included
quadratic	3.009(6)	0.015(2)	0.00013(19)	99.3	La, Lu omitted
linear[b]	3.100(6)	0.0135(8)		97.4	La, Lu included
linear	3.006(3)	0.0137(5)		99.3	La, Lu omitted

[a] $d(\text{Ln}-\text{Se}) = A_0 - A_1 n + A_2 n^2$. [b] $d(\text{Ln}-\text{Se}) = B_0 - B_1 n$.

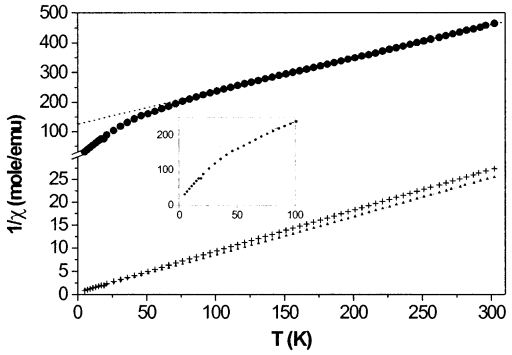

Figure 3. Plots of the inverse magnetic susceptibilities ($1/\chi$) vs T for $RbCeSe_2$ (●), $RbTbSe_2$ (▲), and $RbErSe_2$ (+). The inset provides a closer view of the deviation of $1/\chi$ for $RbCeSe_2$ from Curie−Weiss behavior.

Table 4. Results of Magnetic Measurements on $RbLnSe_2$ (Ln = Ce, Tb, Er)

cmpd	C (emu K/mol)	θ_p (K)	μ_{eff} (μ_B), obsd	μ_{eff} (μ_B), theory[a]
$RbCeSe_2$	0.896	−113.1	2.68	2.54
$RbTbSe_2$	11.97	−2.58	9.78	9.72
$RbErSe_2$	11.22	−4.80	9.47	9.59

[a] Ref 39.

lacking spherical symmetry.[37] In the present instance, spherically symmetric Gd^{3+} ($4f^7$) appears to obey the linear expression.

Magnetic Susceptibilities. Plots of the reciprocal of the molar susceptibility ($1/\chi$) versus T for $RbCeSe_2$, $RbTbSe_2$, and $RbErSe_2$ are shown in Figure 3. $RbTbSe_2$ and $RbErSe_2$ show Curie−Weiss paramagnetic behavior between 5 and 300 K. $RbCeSe_2$ shows similar behavior between 100 and 300 K. The results of least-squares fitting of the paramagnetic regions are given in Table 4. The effective magnetic moments are close to the theoretical values[39] because the 4f-electrons are well localized. This provides justification for treating the 4f-electrons as core electrons in the electronic structure calculations. For most alkali-metal rare-earth chalcogenides, the values of θ_p are small because the exchange interactions are weak in these semiconductors. For $RbCeSe_2$, the Weiss constant is very negative, and at lower temperatures its reciprocal susceptibility deviates from the Curie−Weiss line, as indicated in the inset of Figure 3. Such a deviation has also been observed in other cerium compounds[10,40] and can be attributed to crystal-field splitting of the $^2F_{5/2}$ Ce^{III} ground state.[41]

(39) Kittel, C. *Introduction to Solid State Physics*, 6th ed.; Wiley: New York, 1986.
(40) Wu, P.; Christuk, A. E.; Ibers, J. A. *J. Solid State Chem.* **1994**, *110*, 337−344.
(41) Duczmal, M.; Pawlak, L. *J. Magn. Magn. Mater.* **1988**, *76*−*77*, 195−196.

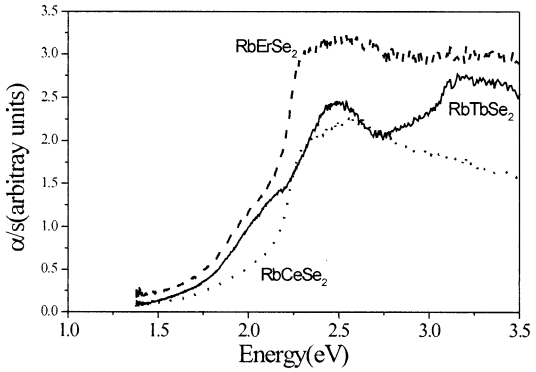

Figure 4. Diffuse reflectance spectra of $RbCeSe_2$, $RbTbSe_2$, and $RbErSe_2$.

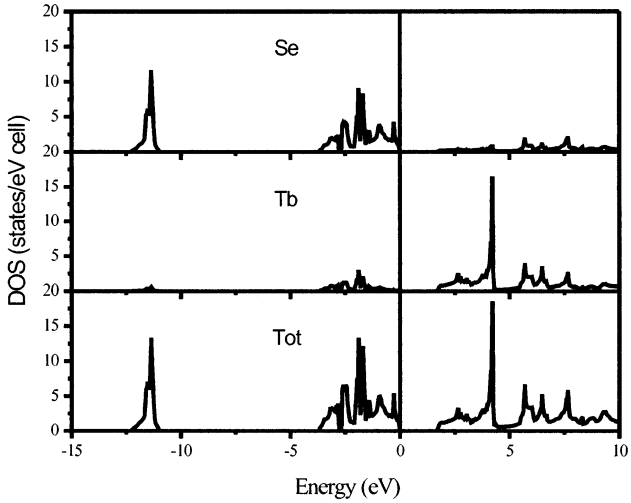

Figure 5. Density of states of $RbTbSe_2$.

Band Gaps and Electronic Structure. The colors of the $RbLnSe_2$ compounds range from red to yellow; band gaps around 2.0 eV are therefore expected. The diffuse reflectance spectra for $RbCeSe_2$, $RbTbSe_2$, and $RbErSe_2$ are depicted in Figure 4. The band gaps for these compounds are between 2.0 and 2.2 eV.

Because all the 4f-electrons were frozen during the TB-LMTO calculations, the electronic structures of the $RbLnSe_2$ compounds are very similar. Here, we discuss the electronic structure of $RbTbSe_2$, as a typical example. The band gap at the Γ point is about 2.5 eV, consistent with the optical measurements. The indirect gap from Γ to L is 1.8 eV. Figure 5 shows the density of states of $RbTbSe_2$. The Se 4p-electrons contribute considerably to the DOS near the Fermi level, whereas the Rb electrons contribute minimally. Most of the contributions in the conduction band are from Tb. From the band structure, we find that the band gap originates from the interactions between Ln and Se. The optical absorption in these compounds can thus be assigned to the transition from mainly a Se^{2-} valence band to mainly a Ln^{3+} conduction band. For comparison with $RbTbSe_2$, we also performed calculations on $RbTbS_2$. Here, the band gap at the Γ point is 3.1 eV, and the indirect band gap from Γ to L is 2.1 eV. Because the sequence of energy levels of p orbitals is 2p(O) < 3p(S) < 4p(Se) < 5p(Te), it should, in principle, be possible to tune the band gap in the series $ALnQ_2$ through

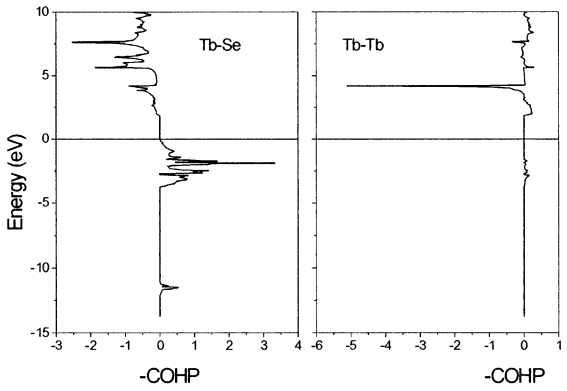

Figure 6. Crystal orbital Hamiltonian populations (COHP) in $RbTbSe_2$. A positive value at a specific energy implies that the states are bonding, and a negative value implies that the states are antibonding.

choice of Q (=O, S, Se, Te). Finer tuning can probably be achieved by change of Ln or A (=Li, Na, K, Rb, Cs), similar to the fine-tuning of the optical band gaps in the $ALnMSe_3$ compounds.[42]

(42) Mitchell, K.; Haynes, C. L.; McFarland, A. D.; Van Duyne, R. P.; Ibers, J. A. *Inorg. Chem.* **2002**, *41*, 1199−1204.

The magnitude of covalent bonding can be deduced from the COHP curves shown in Figure 6. Because the Rb−Se overlap population at the Fermi level is very small (not shown in Figure 6), the Rb−Se bond has more ionic character than covalent character. On the other hand, the Tb−Se bond is largely covalent. Note also that the Tb···Tb interaction is weak. This is consistent with the magnetic measurements, which provide no indication of magnetic ordering.

Acknowledgment. This research was supported by the U.S. National Science Foundation under Grant DMR00-96676 (J.A.I.), by the U.S. Department of Energy under Grant F602•84ER45097 (D.E.E.), and by the MRSEC program of the National Science Foundation (DMR00-76097) at the Materials Research Center of Northwestern University. We also thank Dr. Richard Dronskowski of the Aachen University of Technology for providing the COHP program.

Supporting Information Available: Crystallographic information in CIF format for $RbLnSe_2$ (Ln = La, Ce, Pr, Nd, Sm, Gd, Tb, Ho, Er, Lu). This material is available free of charge via the Internet at http://pubs.acs.org.

IC020324J